Four-body model for transfer excitation

A. L. Harris, J. L. Peacher, and D. H. Madison
Physics Department, Missouri University of Science and Technology, Rolla, Missouri 65401, USA

J. Colgan
Theoretical Division, Los Alamos National Laboratory, Los Alamos, New Mexico 87545, USA
(Received 26 August 2009; published 3 December 2009)

We present here a four-body model for transfer-excitation collisions, which we call the four-body transfer-excitation (4BTE) model. Each two-body interaction is explicitly included in the 4BTE model, allowing us to study the effects of individual two-body interactions. We apply our model to fully differential cross sections for proton+helium collisions, and study the effect of the incident projectile-atom interaction, the scattered projectile-ion interaction, the projectile-nuclear interaction, and electron correlation within the target atom.

DOI: 10.1103/PhysRevA.80.062707 PACS number(s): 34.50.−s, 34.70.+e

I. INTRODUCTION

Four-body atomic collisions present vast opportunities for the study of many particle dynamics, and have been studied for decades in the context of total cross sections. Recent experimental advancements now allow for the measurement of kinematically complete fully differential cross sections (FDCS) [1–22], which present more stringent tests of theoretical models. One of the simplest four-body collisions is a charged particle collision with a helium atom. In this case, two atomic electrons undergo a transition, and electron-electron correlation would be expected to play an important role.

In this paper, we study the four-body process of proton +helium transfer excitation (TE). In this process, an incident proton captures one electron from the target helium atom and leaves the collision as a hydrogen atom. The remaining electron in the helium ion is promoted to an excited state. This is an attractive four-body process to study because the final state contains no continuum electrons, avoiding the complications that are present in some other four-body processes.

For FDCS, the TE process has been studied very little, with only two sets of experimental results, and one theoretical model reported in the literature. The theoretical model is that of Kirchner [21,22], and the experiments are those of Hasan *et al.* [21] and Schöffler [23]. Kirchner's model is a semiclassical, nonperturbative, impact parameter model that employs the independent electron approximation. Experimental absolute differential cross sections for TE show little structure, while Kirchner's theory predicts some structure. This predicted structure is not unique to the TE process, but also occurs in differential cross section calculations for single transfer without excitation [24–26] where experiment again shows little structure. For single charge transfer without excitation, this structure is typically attributed to a cancellation of terms in the perturbation potential. For TE, the structure has been partially, but not entirely, attributed to the nuclear-nuclear interaction [27,28].

We introduce here the four-body transfer-excitation (4BTE) model, which is a fully quantum mechanical four-body model. It explicitly takes into account each particle and interaction in the collision, allowing for a systematic study of the dynamics of the process. To do this, the T matrix is evaluated by computing a nine-dimensional integral numerically. In this paper, we study the role of the incident projectile-target atom interaction, the scattered projectile-residual ion interaction, the projectile-nuclear interaction, and target atom correlation. Atomic units are used throughout.

II. 4BTE THEORY

The FDCS for transfer-excitation is differential only in the projectile scattering angle, and can be written as

$$\frac{d\sigma}{d\Omega} = (2\pi)^4 \mu_{pa}\mu_{hi}\frac{k_f}{k_i}|T_{fi}|^2, \tag{1}$$

where μ_{pa} is the reduced mass of the projectile and target atom, μ_{hi} is the reduced mass of the outgoing hydrogen and residual He^+ ion, and $\vec{k}_i$ ($\vec{k}_f$) is the momentum of the incident (scattered) projectile.

In the two potential formulation, the exact transition matrix T_{fi} is given by [29]

$$T_{fi} = \langle \chi_f^{(-)}|V_i|\beta_i\rangle + \langle \chi_f^{(-)}|W_f^{\dagger}|(\Psi_i^{(+)} - \beta_i)\rangle, \tag{2}$$

where $\chi_f^{(-)}$ is an approximate final state wave function, $\Psi_i^{(+)}$ is the exact initial state wave function, and β_i is the asymptotic initial state wave function. The final state perturbation is W_f, and the initial state projectile-atom interaction is V_i. It is given by

$$V_i = \frac{Z_p Z_{nuc}}{r_1} + \frac{Z_p Z_e}{r_{12}} + \frac{Z_p Z_e}{r_{13}}, \tag{3}$$

where r_1, r_{12}, and r_{13} are the distances from the projectile to the nucleus and two atomic electrons respectively. The quantities Z_p, Z_e, and Z_{nuc} are the electric charges of the projectile, electron, and target nucleus.

The calculations are performed in the center of mass frame, using the Jacobi coodinates [30] shown in Figs. 1 and 2.

In this coordinate system, $\vec{R}_i$ is the relative vector between the incident projectile and the center of mass of the helium atom, and $\vec{R}_f$ is the relative vector between the center of mass

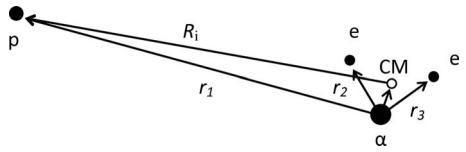

FIG. 1. Jacobi coordinate system for the projectile-helium atom system.

of the hydrogen atom and the center of mass of the He^+ ion. They are given by

$$\vec{R}_i = \vec{r}_1 - \frac{m_e}{m_\alpha + 2m_e}(\vec{r}_2 + \vec{r}_3) \tag{4}$$

and

$$\vec{R}_f = \frac{m_e\vec{r}_2 + m_p\vec{r}_1}{m_p + m_e} - \frac{m_e}{m_e + m_\alpha}\vec{r}_3, \tag{5}$$

where m_e, m_α, and m_p are the masses of the electron, alpha particle, and projectile respectively.

The approximation we use for the final state wave function is

$$\chi_f^{(-)} = \chi_p^f(\vec{R}_f)\phi_H(\vec{r}_{12})\psi_{He^+}(\vec{r}_3), \tag{6}$$

where $\chi_p^f(\vec{R}_f)$ is the outgoing hydrogen wave function, $\psi_{He^+}(\vec{r}_3)$ is the final state He^+ wave function, and $\phi_H(\vec{r}_{12})$ is the hydrogen atom wave function. Both $\phi_H(\vec{r}_{12})$ and $\psi_{He^+}(\vec{r}_3)$ are hydrogenic wave functions, and thus known exactly. The final state wave function has been properly symmetrized in the calculations, but the electrons have been labeled here for clarity.

For the outgoing hydrogen atom, either a plane wave given by

$$\chi_p^f(\vec{R}_f) = \frac{e^{i\vec{k}_f\cdot\vec{R}_f}}{(2\pi)^{3/2}} \tag{7}$$

or a Coulomb wave given by

$$\chi_p^f(\vec{R}_f) = \frac{e^{i\vec{k}_f\cdot\vec{R}_f}}{(2\pi)^{3/2}}e^{-\pi\gamma/2}\Gamma(1 - i\gamma) \times {}_1F_1(i\gamma, 1, -i(k_f R_f + \vec{k}_f\cdot\vec{R}_f)) \tag{8}$$

is used, where $\gamma = \frac{Z_p Z_{He^+}}{v_H}$. The quantity Z_{He^+} is the electric charge of the He^+ ion, and v_H is the speed of the outgoing hydrogen atom.

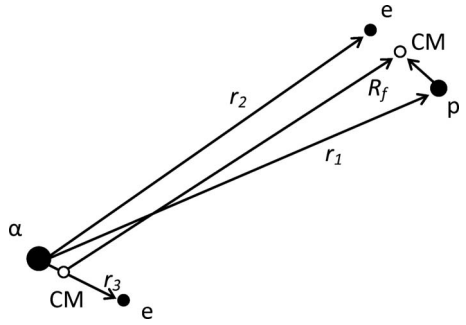

FIG. 2. Jacobi coordinate system for the hydrogen-helium ion system.

We approximate the exact initial state wave function as

$$\Psi_i^{(+)} = \chi_p^i(\vec{R}_i)\xi_{He}(\vec{r}_2, \vec{r}_3), \tag{9}$$

where $\chi_p^i(\vec{R}_i)$ is an incident projectile wave function and $\xi_{He}(\vec{r}_2, \vec{r}_3)$ is the ground-state helium atom wave function.

For the ground-state helium atom, either an analytic Hartree-Fock [31] wave function or a 20-term Hylleraas [32] wave function is used. The Hartree-Fock wave function has no electron-electron correlation, while the Hylleraas wave function contains both radial and angular correlation.

For the incident projectile wave function, either a plane wave given by

$$\chi_p^i(\vec{R}_i) = \frac{e^{i\vec{k}_i\cdot\vec{R}_i}}{(2\pi)^{3/2}} \tag{10}$$

or an Eikonal wave function [33] given by

$$\chi_p^i(\vec{R}_i) = \frac{e^{i\vec{k}_i\cdot\vec{R}_i}}{(2\pi)^{3/2}}\exp\left[i\frac{Z_p}{v_p} \times \ln\left(\frac{(v_p r_1 - \vec{v}_p\cdot\vec{r}_1)^{Z_{nuc}}}{(v_p r_{12} - \vec{v}_p\cdot\vec{r}_{12})(v_p r_{13} - \vec{v}_p\cdot\vec{r}_{13})}\right)\right] \tag{11}$$

is used, where $\vec{v}_p$ is the velocity of the incident projectile.

Since the asymptotic form of the exact initial state wave function β_i is a plane wave times an atomic wave function ξ, using the plane wave of Eq. (10) in the approximate $\Psi_i^{(+)}$ of Eq. (9) causes the second term in the T matrix of Eq. (2) to vanish. The T matrix then reduces to

$$T_{fi}^{PW_i} = \langle\chi_f^{(-)}|V_i|\beta_i\rangle. \tag{12}$$

In terms of perturbation theory, the first term in Eq. (2) represents first order and the second term represents all higher order terms. Consequently, when we use the Eikonal wave function, we are getting parts of all higher order terms in perturbation theory.

The final state perturbation W_f needed for the Eikonal calculation is given by [29]

$$W_f = \frac{1}{\chi_f^{(-)}}(H - E)\chi_f^{(-)}, \tag{13}$$

where H is the full Hamiltonian

$$H = -\frac{1}{2\mu_{pa}}\nabla_{r_1}^2 - \frac{1}{2}\nabla_{r_2}^2 - \frac{1}{2}\nabla_{r_3}^2 + \frac{2}{r_1} - \frac{2}{r_2} - \frac{2}{r_3} - \frac{1}{r_{12}} - \frac{1}{r_{13}} + \frac{1}{r_{23}}, \tag{14}$$

E is the total energy

$$E = \frac{k_f^2}{2\mu_{pa}} + B_H + B_{He^+}, \tag{15}$$

and the final state wave function $\chi_f^{(-)}$ is given by Eq. (6). The quantities B_H and B_{He^+} are the binding energies of the hydrogen atom and He^+ ion, respectively.

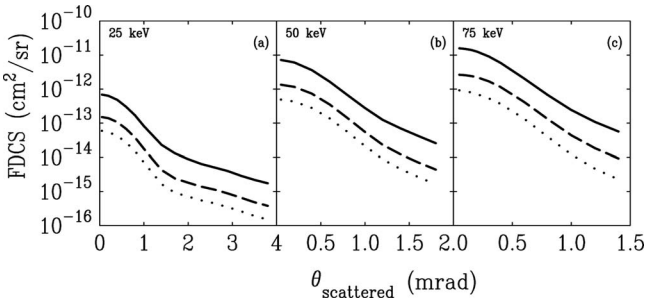

FIG. 3. FDCS as a function of the laboratory projectile scattering angle for p+He TE showing the relative magnitudes of excitation to different energy levels in the He^+ ion. All theoretical curves are from the 4BTE model with a plane wave for the incident projectile, Hylleraas wave function for the helium atom, and Coulomb wave for the scattered projectile. Theoretical results:—excitation to the $n=2$ level; - - - excitation to the $n=3$ level; ⋯ excitation to the $n=4$ level.

Because the evaluation of W_f depends on the final state wave function $\chi_f^{(-)}$, we must calculate W_f for both a plane wave and Coulomb wave, the two scattered projectile wave functions considered here. Evaluating W_f for a plane wave in the final state gives

$$W_f^{PW} = \frac{2 - r_{12}}{2\mu_{pa} r_{12}} + i\frac{\vec{k_f}\cdot\vec{r_{12}}}{\mu_{pa} r_{12}} + \left(\frac{2}{r_1} - \frac{2}{r_2} - \frac{1}{r_{13}} + \frac{1}{r_{23}}\right). \quad (16)$$

For a Coulomb wave in the final state, the final state perturbation is given by

$$\begin{aligned} W_f^{CW} = & -\frac{\gamma k_f}{\mu_{pa}} \frac{{}_1F_1(1+i\gamma,1;-ik_f r_1 - i\vec{k_f}\cdot\vec{r}_1)}{{}_1F_1(i\gamma,1;-ik_f r_1 - i\vec{k_f}\cdot\vec{r}_1)} \\ & + \frac{{}_1F_1(1+i\gamma,2;-ik_f r_1 - i\vec{k_f}\cdot\vec{r}_1)}{{}_1F_1(i\gamma,1;-ik_f r_1 - i\vec{k_f}\cdot\vec{r}_1)} \\ & \times \left[\frac{\gamma k_f}{\mu_{pa}}(\hat{k}_f + \hat{r}_1)\cdot\frac{\vec{r_{12}}}{r_{12}} - i\frac{\gamma k_f}{\mu_{pa}}\vec{k_f}\cdot(\hat{k}_f + \hat{r}_1)\right] \\ & + \frac{2 - r_{12}}{r_{12}} + \left(\frac{2}{r_1} - \frac{2}{r_2} - \frac{1}{r_{13}} + \frac{1}{r_{23}}\right) + i\frac{\vec{k_f}\cdot\vec{r_{12}}}{\mu_{pa} r_{12}}. \end{aligned} \quad (17)$$

III. RESULTS

Currently, experimental data for fully differential cross sections are available for proton+helium transfer excitation collisions at projectile energies of 25, 50, and 75 keV. The experiment was performed by Hasan *et al.* [21], and is absolute. From experiment, it is known that the outgoing hydrogen atom is in the ground state, and the residual helium ion is in an excited state. However, it is not known in which excited state the helium ion is left. Therefore, the cross sections must be summed over all possible excited states. Figure 3 shows the relative magnitude of leaving the helium ion in the $n=2$, 3, or 4 excited states. As can be seen, the $n=4$ contributions are more than an order of magnitude smaller than the

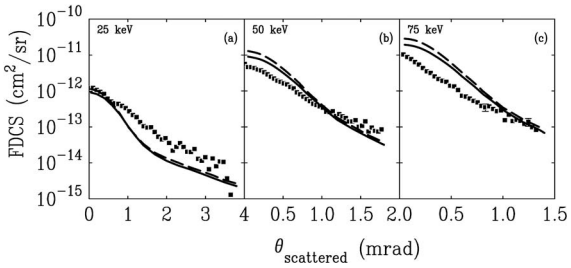

FIG. 4. FDCS as a function of the laboratory projectile scattering angle for p+He TE showing the effect of electron correlation in the target atom wave function. Experiment: ■ results of Hasan *et al.* [21] for the incident projectile energies shown in the figure. Theoretical results:—4BTE model with a plane wave for the incident projectile, Hylleraas wave function for the helium atom, and Coulomb wave for the scattered projectile; - - - 4BTE model with a plane wave for the incident projectile, Hartree-Fock wave function for the helium atom, and Coulomb wave for the scattered projectile.

$n=2$ contribution. Also, for a given energy level, we found that the contribution of leaving the ion in an angular momentum state greater than $l=1$ is negligible. Because of this, the present results include only s and p excited states for $2 \leq n \leq 4$.

In Fig. 4, the effect of initial state electron-electron correlation is shown. One would be inclined to think that correlation would play an important role in a first-order model of a four body process because the only interactions included in the perturbation are between the projectile and each individual electron, as well as the projectile-nuclear interaction. Thus, in order for two electrons to change state, it seems reasonable to expect that some correlation should be required (i.e., the projectile strikes one electron, and the interaction between the two electrons causes the second electron to change state).

Here, two different target helium atom wave functions are used. The Hartree-Fock wave function is a product wave function and contains no correlation. This calculation corresponds to an independent electron model. The Hylleraas wave function includes both radial and angular correlation between the two initial state atomic electrons. Surprisingly, there is very little difference between these calculations, indicating that correlation is not important in this process.

In the final state, the outgoing hydrogen atom is in the field of the He^+ ion. Asymptotically, the ion has a charge of 1, but the hydrogen atom is neutral. This seems to imply that a plane wave should be used for the outgoing hydrogen in order to match asymptotic boundary conditions. However, the dynamics of the collision take place at small projectile-ion separations, so that one might consider the use of a Coulomb wave for the proton in the field of the He^+ ion (i.e., a Coulomb wave with charge 1). Results for both of these approximations are shown in Fig. 5. It is clear that the use of a Coulomb wave is required in order to achieve the correct order of magnitude. However, virtually no change in shape between the two calculations is observed. One might also notice that the difference between the calculations diminishes as projectile energy increases. This is expected since a projectile with a larger speed spends less time in the field of the ion than one with a smaller speed.

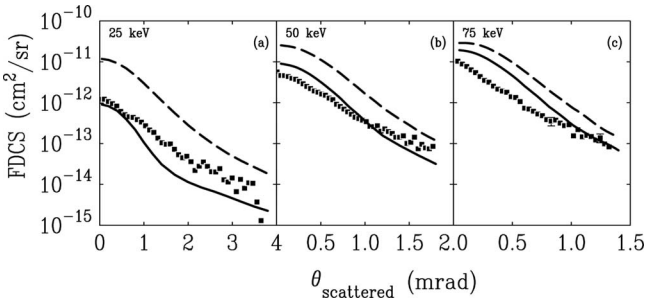

FIG. 5. FDCS as a function of the laboratory projectile scattering angle for p+He TE showing the effect of the scattered projectile-residual ion interaction. Experiment: ■ results of Hasan *et al.* [21] for the incident projectile energies shown in the figure. Theoretical results:—4BTE model with an plane wave for the incident projectile, Hylleraas wave function for the helium atom, and Coulomb wave for the scattered projectile; - - - 4BTE model with a plane wave for the incident projectile, Hylleraas wave function for the helium atom, and plane wave for the scattered projectile.

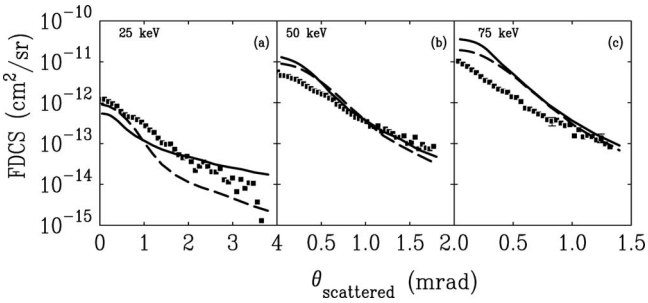

FIG. 6. FDCS as a function of the laboratory projectile scattering angle for p+He TE showing the effect of the incident projectile-target atom interaction. Experiment: ■ results of Hasan *et al.* [21] for the incident projectile energies shown in the figure. Theoretical results:—4BTE model with an Eikonal wave function for the incident projectile, Hylleraas wave function for the helium atom, and Coulomb wave for the scattered projectile; - - - 4BTE model with a plane wave for the incident projectile, Hylleraas wave function for the helium atom, and Coulomb wave for the scattered projectile.

In addition, the use of a Coulomb wave for asymptotic charge 1 changes the asymptotic boundary conditions of the problem, and is likely the reason that agreement with experiment improves at large scattering angles. This is because large scattering angles imply small impact parameters, where the Coulomb interaction between the projectile and ion would be expected to be most important. This improved agreement for large scattering angles seems to imply that the dynamics of the close collisions are more important than the asymptotic boundary conditions. However, we are puzzled by the lack of agreement with experiment at small scattering angles, particularly for the largest projectile energy, where a perturbative model should work best.

Despite the fact that the target atom is neutral, the initial state interaction of the projectile with the constituents of the target atom can be included through the use of an Eikonal initial state wave function. In the Eikonal initial state approximation, the interaction of the projectile with the target nucleus and the atomic electrons is included through a phase factor modifying a plane wave [see Eq. (11)]. This Eikonal phase factor is the asymptotic limit of the Coulomb interaction between the respective particles. Using an Eikonal wave function has the added advantage of including higher order perturbation series contributions.

The Eikonal wave function is typically used for high energy projectiles, and is considered a valid approximation when the ratio Z_{nuc}/v_p is less than 1. For the three energies studied here, this ratio ranges between 1.2 (75 keV) and 2 (25 keV), pushing the limit of the Eikonal's validity. However, even at the lowest energy, use of the Eikonal initial state wave function should be an improvement over a plane wave.

In Fig. 6, the effect of changing the incident projectile wave function from a plane wave to an Eikonal wave function is shown. It is seen that the use of the Eikonal wave function has a fairly small effect for the highest energy, but becomes increasingly important as the energy decreases. For larger scattering angles, the Eikonal wave function increased the cross section, producing better agreement with experiment. This is particularly evident at 25 and 50 keV. The better agreement with experiment for larger scattering angles is expected because a plane wave treatment should become worse with increasing scattering angle. Surprisingly, for small scattering angles, the Eikonal treatment produced worse agreement with experiment at all energies.

As mentioned in the Introduction, for single charge transfer without excitation, inclusion of all three terms in the perturbation potential usually results in some structure (i.e., a minimum) in the FDCS, while excluding the projectile-nuclear term results in a nearly uniform decrease in the cross section. This pronounced change in shape for single charge transfer without excitation prompted us to examine the same effect for transfer excitation. Figure 7 shows the effect of either including or excluding the projectile-nuclear interaction in the perturbation V_i of Eq. (3) on the fully differential cross sections. One would expect that the projectile-nuclear interaction should have a greater effect at large scattering angles, and thus its exclusion from the calculation should

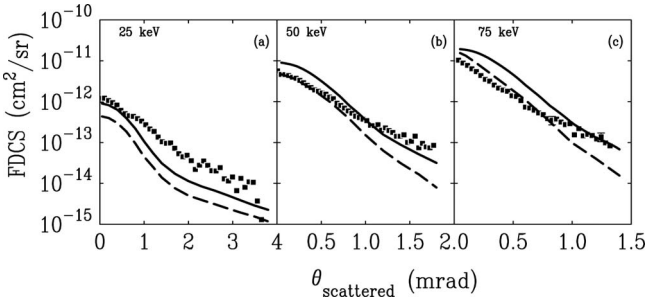

FIG. 7. FDCS as a function of the laboratory projectile scattering angle for p+He TE showing the effect of the projectile-nuclear interaction. Experiment: ■ results of Hasan *et al.* [21] for the incident projectile energies shown in the figure. Both theoretical curves are from the 4BTE model with a plane wave for the incident projectile, Hylleraas wave function for the helium atom, and Coulomb wave for the scattered projectile. Theoretical results:—all three terms in the perturbation; - - - without the projectile-nuclear term in the perturbation.

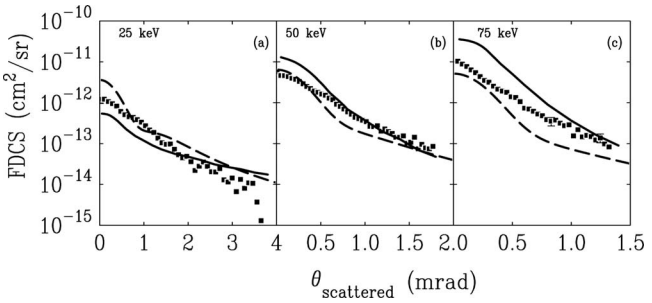

FIG. 8. FDCS as a function of the laboratory projectile scattering angle for p+He TE comparing the 4BTE model with the TC-BGM model [22]. Experiment: ■ results of Hasan *et al.* [21] for the incident projectile energies shown in the figure. Theoretical results:—4BTE model with an Eikonal wave function for the incident projectile, Hylleraas wave function for the helium atom, and Coulomb wave for the scattered projectile; - - - TC-BGM model.

result in a more rapid decrease of the fully differential cross section as scattering angle increases. We found that excluding the projectile-nuclear interaction resulted in a decrease in the cross section, but that this decrease was nearly uniform as a function of scattering angle. Figure 7 also shows that, unlike single capture without excitation, including or excluding the projectile-nuclear term in the interaction potential has little effect on the shape of the FDCS.

One may argue that the nuclear term should be neglected since this term would be zero if the initial and final state wave functions are orthogonal. However, $\chi_f^{(-)}$ and β_i are eigenfunctions of different Hamiltonians, and not necessarily orthogonal. Thus, the nuclear term does not necessarily vanish. Although, neglecting the nuclear term produced improved agreement with experiment for the smaller scattering angles at the two higher energies, we assume that this is fortuitous.

Finally, in Fig. 8, we compare the 4BTE model using an Eikonal wave function for the incident projectile, Hylleraas wave function for the helium atom, and Coulomb wave for the scattered projectile with the two-center-basis generator method (TC-BGM) calculation of Kirchner [22]. The TC-BGM model is based on the impact parameter model, and uses the Eikonal approximation to describe the projectile deflection. It employs the independent electron model, which contains no electron-electron correlation. Overall, the 4BTE model tends to yield better agreement with experiment for the larger scatting angles, and the TC-BGM model tends to do better for small scattering angles. At the two higher energies, both models exhibit a similar shape, with the 4BTE model falling off somewhat more rapidly as scattering angle increases. For all energies, the TC-BGM model exhibits a change in slope at about 0.7 mrad. The 4BTE model predicts a less dramatic change in slope for lower energies, and no noticeable change for the highest energy.

IV. CONCLUSION

We have introduced the four-body transfer-excitation model, and applied it to fully differential cross sections for proton+helium collisions. The effects of target atom electron correlation, the scattered projectile-ion interaction, the incident projectile-atom interaction, and the projectile-nuclear interaction were studied.

Electron correlation in the target atom was studied by comparing results using an uncorrelated helium wave function with those of a fully correlated wave function. Results with and without correlation were nearly identical, showing that electron correlation has a negligible effect in the TE process.

For the projectile-ion interaction, a plane wave and Coulomb wave treatment of the outgoing hydrogen atom were compared. The use of a Coulomb wave for the scattered projectile was necessary to achieve the correct order of magnitude, with its effect diminishing as projectile energy increased. For the projectile-atom interaction, an Eikonal wave function was used to include distortion of the incident projectile wave function by the target atom. The Eikonal treatment gave better agreement with experiment for large scattering angles, and worse agreement for small scattering angles.

Finally, the importance of the projectile-nuclear interaction was studied by either including or excluding this term in the perturbation. Excluding the projectile-nuclear interaction lowered the magnitude of the FDCS slightly, but did not change the shape.

ACKNOWLEDGMENTS

This research was supported by the National Science Foundation (Grant No. PHY-0757749) and TeraGrid resources provided by the Texas Advanced Computing Center (Grant No. TG-MCA07S029). The Los Alamos National Laboratory is operated by Los Alamos National Security, LLC for the National Nuclear Security Administration of the U.S. Department of Energy under Contract No. DE-AC5206NA25396. We would also like to thank Roberto Rivarola, Michael Schulz, and Tom Kirchner for helpful discussions.

[1] V. Mergel, R. Dörner, Kh. Khayyat, M. Achler, T. Weber, O. Jagutzki, H. J. Lüdde, C. L. Cocke, and H. Schmidt-Böcking, Phys. Rev. Lett. **86**, 2257 (2001).

[2] M. S. Schöffler, J. Titze, L. Ph. H. Schmidt, T. Jahnke, N. Neumann, O. Jagutzki, H. Schmidt-Böcking, R. Dörner, and I. Mančev, Phys. Rev. A **79**, 064701 (2009).

[3] S. Bellm, J. Lower, and K. Bartschat, Phys. Rev. Lett. **96**, 223201 (2006).

[4] S. Bellm, J. Lower, K. Bartschat, X. Guan, D. Weflen, M. Foster, A. L. Harris, and D. H. Madison, Phys. Rev. A **75**, 042704 (2007).

[5] C. Dupré, A. Lahmam-Bennani, A. Duguet, F. Mota-Furtado,

P. F. O'Mahony, and C. Dal Cappello, J. Phys. B **25**, 259 (1992).
[6] G. Sakhelashvili, A. Dorn, C. Hohr, J. Ullrich, A. S. Kheifets, J. Lower, and K. Bartschat, Phys. Rev. Lett. **95**, 033201 (2005).
[7] A. Dorn, A. Kheifets, C. D. Schröter, B. Najjari, C. Höhr, R. Moshammer, and J. Ullrich, Phys. Rev. A **65**, 032709 (2002).
[8] M. S. Schöffler, A. L. Godunov, C. T. Whelan, H. R. J. Walters, V. S. Schipakov, V. Mergel, R. Dörner, O. Jagutzki, L. Ph. H. Schmidt, J. Titze, E. Weigold, and H. Schmidt-Böcking, J. Phys. B **38**, L123 (2005).
[9] H. Schmidt-Böcking, V. Mergel, R. Dörner, O. Jagutzki, L. Ph. H. Schmidt, T. Weber, C. L. Cocke, H. J. Lüdde, E. Weigold, Yu V. Popov, H. Cederquist, H. T. Schmidt, R. Schuch, and J. Berakdar, AIP Conf. Proc. **604**, 120 (2001).
[10] H. Schmidt-Böcking, V. Mergel, R. Dörner, C. L. Cocke, O. Jagutzki, L. Schmidt, T. Weber, H. J. Lüdde, E. Weigold, J. Berakdar, H. Ceredquist, H. T. Schmidt, R. Schuch, and A. Kheifets, Europhys. Lett. **62**, 477 (2003).
[11] H. Schmidt-Böcking, V. Mergel, L. Schmidt, R. Dörner, O. Jagutzki, K. Ullmann, T. Weber, H. J. Lüdde, E. Weigold, and A. Kheifets, Radiat. Phys. Chem. **68**, 41 (2003).
[12] X. Ren, A. Dorn, and J. Ullrich, Phys. Rev. Lett. **101**, 093201 (2008).
[13] M. Dürr, A. Dorn, J. Ullrich, S. P. Cao, A. Czasch, A. S. Kheifets, J. R. Götz, and J. S. Briggs, Phys. Rev. Lett. **98**, 193201 (2007).
[14] M. Schulz, D. Fischer, R. Moshammer, and J. Ullrich, J. Phys. B **38**, 1363 (2005).
[15] H. Martinez, F. B. Alarcon, and A. Amaya-Tapia, Phys. Rev. A **78**, 062715 (2008).
[16] A. L. Godunov, C. T. Whelan, H. R. J. Walters, V. S. Schipakov, M. S. Schöffler, V. Mergel, R. Dörner, O. Jagutzki, L. Ph. H. Schmidt, J. Titze, and H. Schmidt-Böcking, Phys. Rev. A **71**, 052712 (2005).
[17] A. Lahmam-Bennani, I. Taouil, A. Duguet, M. Lecas, L. Avaldi, and J. Berakdar, Phys. Rev. A **59**, 3548 (1999).
[18] I. Taouil, A. Lahmam-Bennani, A. Duguet, and L. Avaldi, Phys. Rev. Lett. **81**, 4600 (1998).
[19] A. Dorn, R. Moshammer, C. D. Schröter, T. J. M. Zouros, W. Schmitt, H. Kollmus, R. Mann, and J. Ullrich, Phys. Rev. Lett. **82**, 2496 (1999).
[20] W. T. Htwe, T. Vajnai, M. Barnhart, A. D. Gaus, and M. Schulz, Phys. Rev. Lett. **73**, 1348 (1994).
[21] A. Hasan, B. Tooke, M. Zapukhlyak, T. Kirchner, and M. Schulz, Phys. Rev. A **74**, 032703 (2006).
[22] M. Zapukhlyak, T. Kirchner, A. Hasan, B. Tooke, and M. Schulz, Phys. Rev. A **77**, 012720 (2008).
[23] M. S. Schöffler, Ph.D. thesis, University of Frankfurt am Main, 2006.
[24] P. N. Abufager, P. D. Fainstein, A. E. Martínez, and R. D. Rivarola, J. Phys. B **38**, 11 (2005).
[25] I. Mančev, V. Mergel, and L. Schmidt, J. Phys. B **36**, 2733 (2003).
[26] M. Schulz, T. Vajnai, and J. A. Brand, Phys. Rev. A **75**, 022717 (2007).
[27] K. Omidvar, Phys. Rev. A **12**, 911 (1975).
[28] Dž. Belkić and A. Salin, J. Phys. B **11**, 3905 (1978).
[29] S. Jones and D. H. Madison, Phys. Rev. A **65**, 052727 (2002).
[30] M. R. C. McDowell and J. P. Coleman, *Introduction to the Theory of Ion-Atom Collisions* (North-Holland, Amsterdam, 1970).
[31] F. W. Byron and C. J. Joachain, Phys. Rev. **146**, 1 (1966).
[32] J. F. Hart and G. Herzberg, Phys. Rev. **106**, 79 (1957).
[33] D. S. F. Crothers and J. F. McCann, J. Phys. B **16**, 3229 (1983).